Deciphering the CENTAURO puzzle

Scott Pratt
National Superconducting Cyclotron Laboratory and Department of Physics and Astronomy, Michigan State University, East Lansing, Michigan 48824
(Received 25 February 1994)

The effects of multiboson interference with regard to isospin imbalances and spectra are calculated for high-energy hadronic collisions. Emission is modeled by a relativistic thermal source with a Bjorken geometry. The requirements for creating CENTAURO-like phenomena are explored. It is shown that strong collective Bose effects occur when breakup densities are of the order of one pion per cubic fm. The possibility of emitting pions through isoscalar channels, which can explain large isospin imbalances, is investigated.

PACS number(s): 25.75.+r, 13.85.Tp, 05.30.Jp

I. INTRODUCTION

High-multiplicity cosmic-ray events with anomalous isospin imbalances have been observed for over three decades and are known as CENTAURO events [1]. Most particles from a high-energy event should be pions; therefore one-third of the particles should be neutral pions which should leave electromagnetic signals from the $\pi_0 \rightarrow 2\gamma$ decay. An event without such a component is known as a CENTAURO event while an event with an excess electromagnetic signal, corresponding to an excess of neutral pions, is known as an anti-CENTAURO. This behavior has motivated exotic explanations such as quark nuggets or disordered chiral condensates [2,3].

In 1984 Lam and Lo [4–7] suggested that the large isospin fluctuations were due to the Bose nature of the emitted pions. They considered both the case of emission from a large number of deltas and thermal emission under the constraint that the source equilibrated. Using diagrammatic techniques [8] the same conclusion was obtained for a thermal Gaussian source of finite size emitting according to the symmetrization weights of outgoing particles. Reference [8] demonstrated that such symmetrization enhancements do not require an assumption that a source has somehow equilibrated, which would require a long reaction time, but merely that multiparticle trajectories are weighted by the outgoing multiparticle wave functions. The effect of constraining the emission to isoscalar pairs was investigated [9] it was shown that isospin constraints greatly magnify the effects of symmetrization. The models used in these calculations were schematic and did not incorporate relativistic effects or collective expansion.

In this paper, we report results from a statistical model with a realistic space-time and momentum space description. Emission of hadrons from an energetic collision cannot be well described by a static thermal source. Pions are emitted over several units of rapidity due to the collective flow of the matter, which is a result of incomplete stopping. We apply the techniques of Refs. [8,9] to the case of thermal emission from a Bjorken geometry [10]. The sources emit with thermal weights in their rest frame with the time and position of the emission being given according to the Bjorken geometry, which accounts for collective flow along the beam axis — the correlation between position and momentum. If the distribution of source rapidities was uniform, all measured quantities would be boost invariant. The actual distribution of sources is certainly not boost invariant. We assume the sources have a range of rapidities denoted by Δ, which will be a crucial parameter in our study. We wish to learn for what values of Δ and dN/dy laserlike behavior is expected to occur.

We calculate not only corrected isospin distributions but also the distortion of the single-body spectra. We show that the symmetrization hypothesis for explaining CENTAURO behavior can be tested by searching for simultaneous bunching in rapidity and transverse momenta.

Physical, mathematical, and numerical details of the calculation are laid out in the next section. Symmetrization distortions to spectra are described in the third section. The fourth section contains a detailed discussion of isospin constraints, while modifications of isospin distributions are presented in the fifth section. In the conclusions we assess the possibility that incoherent sources could lead to CENTAURO-like behavior given the bosonic nature of pions and the constraints of isospin conservation.

II. FORMALISM AND METHODS

In Ref. [8] a formalism was developed for calculating symmetrization corrections to all orders for single-body spectra, two-body correlations, multiplicity distributions, and isospin distributions. The technique rests on the assumption that particles are emitted independently and then interfere in their outgoing states, due to Bose symmetrization. Coulomb and strong interactions

are neglected. First we review the formalism. The equations below are somewhat different from those of Refs. [8,9] as they are done in an explicitly Lorentz-invariant manner.

Independent emission implies that the n-particle matrix elements factorize into a product of the one-body elements as shown below in the expression for the Lorentz-invariant n-particle cross section:

$$P(p_1,p_2,...,p_n) = \left| \int d^4x_1 d^4x_2 \cdots d^4x_n T(x_1)\cdot T(x_2)\cdots T(x_n)\; U(x_1,x_2,...,x_n;p_1,p_2,...,p_n) \right|^2 . \tag{2.1}$$

The symmetrized evolution operator $U(x;p)$ has $n!$ terms which can be accounted for diagramatically.

$$U(x_1,...,x_n;p_1,...,p_n) = \sum_{\langle i_1,i_2,...,i_n\rangle} e^{\{ip_1x_{i_1}+ip_2x_{i_2}+\cdots i(p_nx_{i_n}\}}, \tag{2.2}$$

where the sum is over the $n!$ permutations of the integers $1-n$ into i_1-i_n.

This form for the evolution operator U neglects the hadronic interaction between the pions as well as the Coulomb interaction. The effects of Coulomb interaction should largely cancel as the net charge of the system is zero. Hadronic interactions can be important, particularly when the system is dense. Strong interactions manifest themselves largely through resonances such as ρ's, ω's and η's. Pions which are formed through these resonant channels contribute much less to the symmetrization. Formation of pions through isoscalar channels is discussed at great length later in this paper, while a more responsible account of the effects of the other channels will be a topic for future study.

All the physical input comes from assuming a form for $T(x)$. Rather than work with $T(x)$, which is a complex quantity, we work with a more physical quantity, $S(p,x)$, the Wigner transform of $T^\dagger T$:

$$S(p,x) \equiv \int d^4\delta x\; \exp(ip\delta x)\; T^\dagger\left(x+\frac{\delta x}{2}\right) T\left(x-\frac{\delta x}{2}\right). \tag{2.3}$$

If one knew the quantum-mechanical matrix elements $T(x)$, one could find $S(p,x)$ exactly. Detailed knowledge of the quantum-mechanical matrix elements is impossible, therefore one must assume a form of $S(p,x)$ which incorporates the salient space-time features of the emission. Here we have assumed that the matrix elements are Lorentz-invariant quantities (e.g., Lagrangian elements).

The four-momenta p and q are on shell which means that the emission function $S(x,(p+q)/2)$ is evaluated off shell since $E((\mathbf{p}+\mathbf{q})/2)$ does not necessarily equal $[E(\mathbf{p})+E(\mathbf{q})]/2$.

Usually one is interested in quantities where one has integrated over most of the n-particle observables. For example, one might wish to know single-body spectra or the multiplicity distribution. One can write such quantities in terms of simple line diagrams and ring diagrams which are denoted by $G_n(p,q)$ and C_n. The line diagrams of order n consist of a straight line with n dots which break the line into $n+1$ segments. The momenta p and q are associated with incoming and outgoing segments. The intermediate segments are labeled k_2 through k_n and the dots are labeled x_1 through x_n. Associated with each dot is an emission factor $S(\frac{1}{2}(k_1+k_2),x)$ and a phase factor $\exp[i(p-q)x]$. All quantities are constructed from the lowest order diagram G_1,

$$G_1(p,q) = \int d^4x \left(\frac{p+q}{2},x\right) e^{[i(p-q)x]}. \tag{2.4}$$

The nth order line diagrams can be found by convoluting G_1:

$$G_n(p,q) = \int \frac{d^3k_2}{E_2}\frac{d^3k_3}{E_3}\cdots\frac{d_n^k}{E_n} G_1(p,k_2) \times G_1(k_2,k_3)\cdots G_1(k_n,q). \tag{2.5}$$

The ring diagrams C_n can be found by integrating $G_n(p,p)$:

$$C_n = \frac{1}{n}\int \frac{d^3p}{E_p} G_n(p,p). \tag{2.6}$$

Relative symmetrization weights for emitting a number of pions N are given by the sum $\omega(N)$ of all ring diagrams $C(i)$, connected or disconnected, such that the resulting order is N. The algorithm for performing this sum is described in [8]. The sum can be written as follows where i_j refers to the number of time the ring diagram of order j appears in a given diagram:

$$\omega(N) = \prod_{\langle i_1,i_2,\cdots iN,s.t.i_1+2\cdot i_2+\cdots N\cdot i_N=N\rangle} \frac{C_1^{i_1}}{i_1!}\frac{C_2^{i_2}}{i_2!}\cdots\frac{C_N^{i_N}}{i_N!}. \tag{2.7}$$

The differential probability for a pion to be emitted with momentum p from an N-particle event is

$$\frac{E_p d^3P}{dp^3} = \frac{G_1(p,p)\omega(N-1)+G_2(p,p)\omega(N-2)+\cdots G_N(p,p)\omega(0)}{\omega(N)}. \tag{2.8}$$

Assuming a form of $S(p,x)$ all observables can be calculated in closed form given that the integrations required to find C_n and $G_n(p,q)$ can be performed. These integrals can be calculated analytically for nonrelativistic thermal models with simple Gaussian or square-well geometries, but for realistic models the integration must be done numerically.

We assume an emission function consistent with a Bjorken geometry. The Bjorken model describes a thermal source expanding along the beam axis with a velocity gradient $1/\tau_0$. The emission times are chosen to be τ_0 where the times are measured in the local frame of the emitting matter. By constraining the local emission time to be equal to the inverse velocity gradient, the model is invariant to boosts along the beam axis, aside from the constraining of the rapidities of the thermal sources through the stopping parameter Δ described below.

This model incorporates thermal behavior and collective expansion along the beam axis, but neglects several other aspects of the behavior. Usually, a significant fraction of pions emitted in high-energy hadronic collisions come from longer-lived resonances. However, we are exploring whether laserlike behavior is responsible for the high values of dN/dy and the isospin fluctuation, in which case most of the multiplicity is due to the enhancement of high-multiplicity events caused by Bose weighting. It is therefore warranted to consider only the prompt pions as the majority of those emitted in such an event and to consider pions from longer-lived resonances as a small fraction, whose emission is not noticeably enhanced by identical-particle statistics. Of course, even prompt pions are not emitted all at the same proper time τ_0, but that aspect of the emission is accounted for by choosing values of the transverse radius R larger than the actual physical values. Transverse expansion is also absent from this description. The amount of transverse expansion is unknown, but by studying the effects of longitudinal expansion one can infer the consequences of transverse expansion.

$$S(p,x) = p_0' \, e^{-p_0'/T} \, \delta(\tau - \tau_0) \, \exp\left\{-\frac{x^2+y^2}{2\,R^2}\right\} \times \exp\left\{-\frac{(\cosh(\eta)-1)}{\Delta^2}\right\}. \tag{2.9}$$

Here the beam coordinate z and the time t have been replaced by the variables τ and η which are defined as

$$\tau = \sqrt{t^2 - z^2}\,, \quad \eta = \sinh^{-1}(z/\tau). \tag{2.10}$$

The last term in Eq. (2.9) constrains the rapidities of the sources to within Δ of zero. This particular form is a bit more sharply cut off than a Gaussian, and was chosen such that the quantity $G_1(p,q)$ could be found analytically. The primed quantities refer to those measured in the rest frame of the matter at the position z. The matter is assumed to be moving with a relativistic velocity $\gamma v = \sinh(\eta)$. The zeroth component of the four-momentum is given by

$$p_0' = \cosh(\eta)p_0 - \sinh(\eta)p_z. \tag{2.11}$$

The momenta that enter the definition of $S(p,x)$ are evaluated in the local emitting frame, ensuring that $S(p,x)$, $G_n(p,q)$, C_n, and $\omega(n)$ are all Lorentz invariant.

As mentioned above this form of $S(p,x)$ allows $G_1(p,q)$ to be found analytically.

$$G_1(p,q) = \frac{K_1(c)}{c} e^{1/\Delta^2} \times[\alpha(y_p,y_q,m_p,m_q) + \alpha(y_q,y_p,m_q,m_p)] \times e^{-[(p_x-q_x)^2+(p_y-q_y)^2]R^2/2}, \tag{2.12}$$

where

$$\alpha(y_p,y_q,m_p,m_q) = m_p\left(\frac{\cosh(y_p)}{\Delta^2} + a + b\cosh(y_p - y_q)\right)$$

$$c = \sqrt{\frac{1}{\Delta^4} + 2ab\cosh(y_p-y_q) + a^2 + b^2 + 2a\cosh(y_p)/\Delta^2 + 2b\cosh(y_q)/\Delta^2}$$

$$a = m_p\left(\frac{1}{2T} - i\tau_0\right), \quad b = m_q\left(\frac{1}{2T} + i\tau_0\right),$$

y_p and y_q refer to the rapidities of the two particles, and m_p and m_q are the transverse masses.

$$y_p = \sinh^{-1}\left(\frac{p_z}{m_p}\right), \quad m_p = \sqrt{p_x^2 + p_y^2 + m^2}. \tag{2.13}$$

Answers will depend on five quantities: the temperature T, the Bjorken time τ, the transverse size R, the particle number N, and the stopping parameter Δ which was discussed above. All the calculations performed in this paper were done assuming a temperature of 175 MeV which is in the right neighborhood to explain transverse-energy spectra in high-energy collisions. The transverse size R and the Bjorken time τ should be in the neighborhood of 1 – 2 fm for hadron induced collisions. We arbitrarily choose $R = c\tau$ to reduce the parameter space. The breakup density depends on R, τ, and the particle number N. Rather than referring to a source size by R and τ we will refer to the corresponding breakup density, as it allows a clearer understanding for how small of a

system we are considering and it allows comparison of systems with different stopping parameters at the same breakup density.

We are now left with the seemingly straightforward task of calculating the quantities $G_n(p,q)$ and C_n from $G_1(p,q)$, which is known analytically. To calculate $G_n(p,q)$ from Eq. (2.5), one must numerically integrate over $n-1$ internal momenta. For high order diagrams this is more difficult than it first appears because, in order for a combination of the $n-1$ internal momenta to contribute, all n momenta must be within $1/R$ of one another. This means that, for higher order quantities, a random sampling Monte Carlo routine fails. In fact for order $n > 5$ straightforward Monte Carlo methods could not converge in acceptable amounts of CPU time. A Metropolis method, on the other hand, can sample a distribution more intelligently. However, Metropolis algorithms are only good for sampling averages of quantities according to a distribution, and are not so convenient for performing integrals. One can, however, write the integral we are performing as an expectation of the integrand we are interested in, divided by an integrand we know how to integrate analytically. The answer we want can then be written as this expectation multiplied by the integral of the integrand we know how to perform analytically. For example, if the integral I wish to perform is I, which requires integration over n coordinates of $A(k_1,k_2,\ldots,k_n)$, and an integral I, know how to perform is I_0, which is an integral over the same coordinates of $A_0(k_1,k_2,...,k_n)$, I can write I as

$$I = \int dk_1 dk_2 \cdots dk_n A(k), \tag{2.14}$$

$$= I_0 \frac{\int dk_1 dk_2 \cdots dk_n A_0(k) \frac{A(k)}{A_0(k)}}{I_0}$$

$$= I_0 \left\langle \frac{A(k)}{A_0(k)} \right\rangle, \tag{2.15}$$

where

$$I_0 = \int dk_1 dk_2 \cdots dk_n A_0(k) \tag{2.16}$$

and $\langle F \rangle$ refers to the average of F according to the distribution A_0. One can now calculate the expectation in Eq. (2.15) using Metropolis methods, multiply this expectation by I_0, and we are done. The trick is finding a distribution A_0 which is calculable analytically, is sufficiently close to A such that the Metropolis algorithm can be performed in a reasonable time, and never has any regions where A/A_0 becomes large.

For calculating C_n as in Eq. (2.6), the corresponding integrands are

$$A(k) = G_1(k_1,k_2)G_1(k_2,k_3)\cdots G_1(k_n,k_1), \tag{2.17}$$

$$A_0(k) = H(k_1,k_2)H(k_2,k_3)\cdots H(k_n,k_1)\left[G_n(\bar{k},\bar{k})\right]^n, \tag{2.18}$$

where

$$H(p,q) = \exp\{-[(p_x-q_x)^2 + (p_y-q_y)^2]R^2/2 - (y_p-y_q)^2 S^2/2\}. \tag{2.19}$$

The parameter S is chosen such that the procedure converges most efficiently. Since $H(k_i,k_{i-1})$ in the previous equation depends only on the relative coordinates, we can see that I_0 will factorize into an integral over the $n-1$ relative momenta which can be done analytically and an integral over the average momentum $\bar{k}$ which can be done numerically:

$$I_0 = \left[\frac{(2\pi)^{3/2}}{SR^2}\right]^{n-1} \frac{1}{n^{3/2}} \int d\bar{k} \left[G_n(\bar{k},\bar{k})\right]^n. \tag{2.20}$$

Using the procedure outlined above, C_n becomes

$$C_n = I_0 \frac{1}{n} \left\langle \frac{G(k_1,k_2)G(k_2,k_3)\cdots G(k_n,k_1)}{A_0} \right\rangle. \tag{2.21}$$

The Metropolis algorithm consists of averaging the quantity in brackets over a path in momentum space found by taking a random walk whose direction is weighted by A_0.

To obtain $G_n(p,p)$ one follows a similar procedure.

$$G_n(p,p) = I_0 \frac{1}{n} \left\langle \frac{G(k_1,k_2)G(k_2,k_3)\cdots G(k_n,k_1)}{A_0} \times \{\delta(p-k_1)+\delta(p-k_2)+\delta(p-k_3)\cdots\} \right\rangle. \tag{2.22}$$

By inspecting Eq. (2.22) one sees that calculating G_n can be performed during the calculation of C_n by simply testing whether any of the momenta are in the neighborhood of p.

Using this procedure, $G_n(p,p)$ and C_n were calculated satisfactorily for values of n up to around 10. Beyond $n = 10$ fluctuations grow such that C_{20} required several hours of CPU time and was still uncertain by a factor of 2. Values of C_n for n greater than 10 were found by extrapolating from the values with n from 6 to 10. The form of the extrapolation was taken from the analytic solution to the nonrelativistic case solved in [8] which closely resembles an exponential in n. The fit of the two-parameter extrapolation to the numerically determined values for n greater than 5 and less than 10 is shown in Fig. 1. The numerically determined value C_{20} is also shown on the figure, illustrating the success of the extrapolation. To extrapolate to higher values of n in the calculation of $G_n(p,p)$ the fitting function was an exponential in n with parameters a and b, $G_n = a\exp(-bn)$.

Diagrams of higher order were responsible for a large portion of the answer, which makes one cautious in the extrapolations. However, in testing many different fitting procedures, the choice of procedure never had more effect than changing R and τ by a few percent. Thus, given the extreme sensitivity to the R and τ_0 parameters which are uncertain on the order of 25%, the extrapolations are satisfactory.

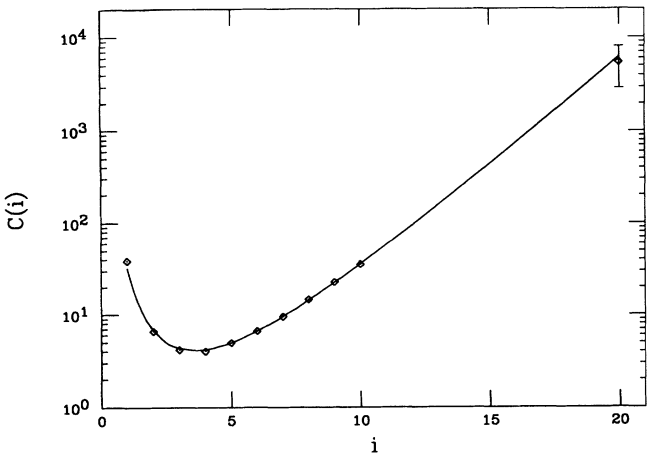

FIG. 1. The closed diagrams $C(i)$ of a given order i. This was performed for the example of $\Delta = 3.0$, $R = c\tau = 1.22$ fm. Due to numerical limitations, higher order diagrams cannot be calculated numerically and must be interpolated from lower order diagrams. Numerically calculated diagrams are shown by diamonds, while the interpolation is shown by the solid line. The two-parameter interpolation, which was fitted for values of i from 6 to 10, is used to obtain values of $C(i)$ for i greater than 10. The interpolation is justified by the comparison of the interpolated value to the numerically determined value at $i = 20$. Numerical fluctuations of $C(i)$ for values of i less than or equal to 10 are smaller than the size of the symbols.

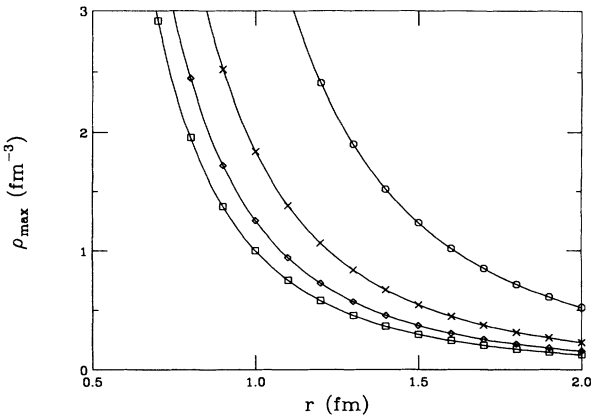

FIG. 2. The maximum density given 60 pions distributed with a transverse radius R and a proper time $c\tau = R$ for several values of the stopping parameter Δ. Small values of Δ confine the emitting sources to a small region of rapidity. The density at the origin is shown for Δ =1.0 (circles), 3.0 (crosses), 6.0 (diamonds), and 10.0 (squares).

III. SINGLE-PARTICLE SPECTRA

Bose symmetrization enhances emission of low-energy particles. The most fundamental example of such effects is the difference of Planck's blackbody spectrum with respect to an exponential. Symmetrization distortions for a finite system with fixed particle number were calculated analytically in the context of a simple model in [8,9]. This model was a nonrelativistic source of Gaussian extent in space and instantaneous in time. The most important characteristic of high-energy collisions which was missing in the analytically solvable model is the lack of collective expansion. This is addressed in the Bjorken-like model described in the previous section, where there is expansion along the beam axis, and the expansion is described by a velocity gradient $1/\tau_0$.

For all the calculations described in this paper the assumed temperature is 175 MeV. Symmetrization effects depend critically on the values of R and τ. All the calculations shown here will assume $R = \tau$; therefore the density scales as R^{-3}. For a given multiplicity, the density is also determined by Δ. The overall extent of the source in the beam direction scales as $\tau\Delta$ for small values of Δ. Rather than referring to values of R and τ we refer to calculations by the resulting breakup density at the origin, $\rho_{\max}$. Thus when we compare symmetrization effects for different values of the stopping parameter Δ we compare for the same $\rho_{\max}$. This means that larger values of Δ will be using smaller values of R and τ to attain the same $\rho_{\max}$. Figure 2 illustrates how $\rho_{\max}$ depends on $R = c\tau$. One should remember that $\rho_{\max}$ refers to the breakup density at the origin and that average breakup densities are less.

Symmetrization corrections to dN/dy are shown in Fig. 3. Normalized to unity, the rapidity distributions for several values of the stopping parameter Δ are shown in Fig. 3(a) with the effects of symmetrization neglected. A 250 TeV cosmic ray has a rapidity of approximately 13. Choosing $\Delta = 10$ corresponds to very little stopping as the resulting dN/dy extends ± 6 units of rapidity. Choosing $\Delta = 1$ corresponds to nearly complete stopping and would be signaled by nearly all the pions being emitted into the central 3 – 4 units of rapidity.

Figure 3(b) illustrates the effects of symmetrization on the stopping. For this example, R and τ were chosen such that sixty pions would result in $\rho_{\max} = 1.0$ fm^{-3}. CENTAURO events might have multiplicity somewhat exceeding 60, but some fraction of those would be emitted from high-energy jets or from long-lived resonances, and their spectra would not be affected by symmetrization. The effects of symmetrization will vary as to whether one is measuring an overpopulated or underpopulated isospin species. For this example, corrections were calculated assuming one is viewing an overpopulated species where 40 of the 60 pions have been emitted with that isospin.

From comparing Fig. 3(b) to Fig. 3(a), one sees that symmetrization enhances the apparent stopping of the collision, but not by so much as to constitute a signal. Estimates of stopping for a high-energy hadron incident on a nuclear target vary widely [11–13].

The transverse-momentum distribution is also distorted by symmetrization, with the greatest amount of distortion occurring for rapidities near zero in the center of mass. Looking at a narrow slice in rapidity, the probability that a pion has a given transverse momentum is shown in Fig. 4. Again it is assumed that the dominant species is measured, and that 40 of 60 pions have that isospin. For this example Δ was set equal to 3.0.

The strength of the distortion depends on the breakup density. Figure 4 illustrates that the distortion becomes strong when ρ_{max} approaches 1.0 fm^{-3} and that the effect saturates for higher breakup densities.

A drop in the mean transverse momentum from expected values in the neighborhood of 450 MeV/c to 300 MeV/c would seem to be a clear signal of strong symmetrization effects, but transverse expansion could easily erase the necessity of a low mean transverse momentum. However, if symmetrization effects are strong, the spectrum for the dominant pion species should differ from that of the underpopulated species. In Fig. 5, the mean transverse momentum is shown as a function of the rapidity assuming one is viewing the overpopulated flavor containing 40 of the 60 pions, an average-populated species containing 20 of the 60 pions, or a strongly underpopulated species. For large y, where the phase-space density is low, the mean p_t becomes identical for all flavors.

From these calculations of the spectra, a clear conclusion can be reached regarding whether CENTAURO phe-

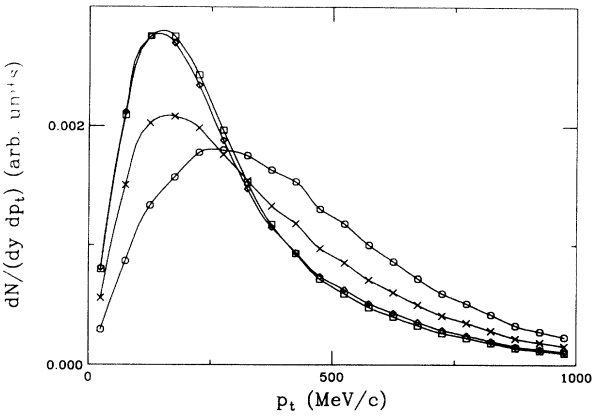

FIG. 4. The transverse-momentum distribution for pions of a given flavor with zero rapidity. Distributions due to 40 pions being emitted with $\Delta = 3.0$ are shown for four values of the maximum density. The base distribution (circles) where symmetrization is neglected would correspond to low densities. For densities of 0.5, 1.0, and 1.5 fm^{-3}, the distributions are denoted by crosses, diamonds, and squares, respectively. Symmetrization causes a strong enhancement at low p_t which strengthens for higher densities.

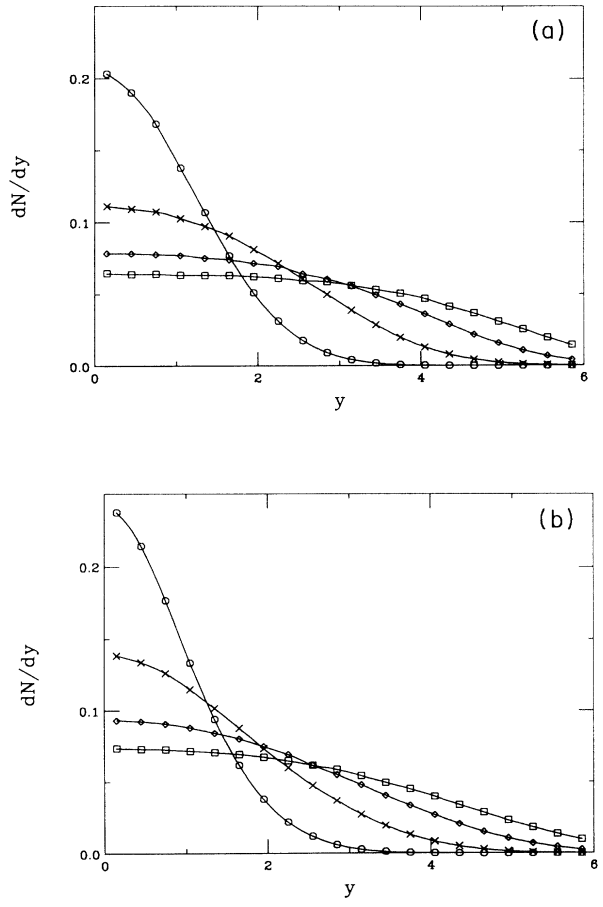

FIG. 3. Rapidity distributions where symmetrization has been neglected are shown in (a). The four values of Δ used are 1.0, 3.0, 6.0, and 10.0 and are represented by circles, crosses, diamonds, and squares, respectively. Smaller values of Δ correspond to greater amounts of stopping, while the largest value yields a rapidity distribution as broad as the incoming rapidity of a 200 TeV cosmic ray. The same distributions are shown in (b), but the effects of symmetrization have been included. The distributions have more apparent stopping, but the enhancement is small compared to the theoretical uncertainty in the stopping due to other effects such as secondary collisions. The proper time τ and the transverse radius R were chosen such that the maximum breakup density was 1.0 fm^{-3}.

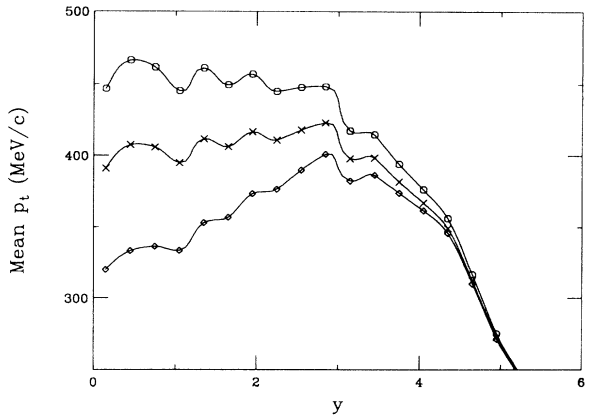

FIG. 5. The mean transverse momentum for pions of a given flavor as a function of their rapidity. Calculations were performed assuming 20 (crosses) or 40 (diamonds) pions were emitted with $\Delta = 3.0$. The base distribution (circles) results from neglecting symmetrization. Including symmetrization lowers the mean transverse momentum, but only at midrapidity. If symmetrization brings on low-p_t enhancement, the enhancement should disappear for rapidities with smaller dN/dy as well as for pions of an underpopulated flavor. Small-scale fluctuations are due to the Monte Carlo nature of the calculation.

nomena are caused by symmetrization. If symmetrization is the cause, Bose distortions to spectra should be different for overpopulated and underpopulated flavors. However, such behavior would not prove that the effect was caused by incoherent sources emitting into outgoing symmetrized wave functions. A coherent component would also likely be focused at low momentum.

It is doubtful that cosmic-ray experiments will provide the statistics necessary for detailed studies of spectra. The possibility of creating such phenomena with accelerator-based experiments is discussed in the conclusion.

IV. CONSTRAINING EMISSION TO ISOSCALAR PAIRS

It was shown in Ref. [9] that symmetrization can explain broadened isospin distributions, but explaining events with very large isospin imbalances requires assumptions regarding isospin constraints. It was shown that, by assuming that emitting N pions factorized into the emission of $N/2$ isoscalar pairs, events with a large isospin imbalance become common. Before discussing the results of the calculations, I review the motivation for constraining the isospin compositions.

In a CENTAURO event where the nucleon-nucleon center-of-mass energy is in the neighborhood of 600 GeV, most produced particles at midrapidity originate from gluons [14]. At this energy a nucleon's structure function might contain 20 gluons with energies greater than 1 GeV. All pions arising from such collisions must be in an isosinglet, and since g-parity is conserved only an even number of pions can be emitted. A typical pion multiplicity from gluons hadronizing might be 4 or 6. Other processes that radiate pions such as Pomerons or a σ field might also tend to radiate a small number of pions in an isosinglet. If a quark-gluon plasma was created with an equilibrium quark composition, the isosinglet constraint would be over a much larger fraction of the distribution. We wish to study the importance of performing the isospin constraint pairwise as was done in Ref. [9], four at a time, or over the entire distribution.

For the example of two pions emitted in an isosinglet, there is only one possible form for the isospin portion of the outgoing wave function:

$$|s2\rangle = |(\vec{a}\cdot\vec{b})\rangle. \tag{4.1}$$

The vector indices refer to the three isospin states while a and b denote the outgoing momentum states. It assumed that we are working in the "$xy0$" basis rather than the "$+-0$" basis. We only calculate observables based on the total pion number and the number of neutral pions, which are not affected by the choice of basis. The "$xy0$" basis is more convenient as all three flavors are treated on an equal footing. The state is normalized given the choice $\langle a_x^\dagger a_x\rangle = 3^{-1/2}$. For the case where four pions are emitted there are three forms:

$$\begin{aligned}
|s_4\rangle &= \frac{1}{\sqrt{Z_s}}\Big\{|(\vec{a}\cdot\vec{b})(\vec{c}\cdot\vec{d}) + (\vec{a}\cdot\vec{c})(\vec{b}\cdot\vec{d}) \\
&\quad +(\vec{a}\cdot\vec{d})(\vec{b}\cdot\vec{c})\rangle\Big\}, \\
|t_4\rangle &= \frac{1}{\sqrt{Z_t}}\Big\{|2(\vec{a}\cdot\vec{b})(\vec{c}\cdot\vec{d}) \\
&\quad -(\vec{a}\cdot\vec{c})(\vec{b}\cdot\vec{d}) - (\vec{a}\cdot\vec{d})(\vec{b}\cdot\vec{c})\rangle\Big\}, \\
|u_4\rangle &= \frac{1}{\sqrt{Z_u}}\Big\{|(\vec{a}\cdot\vec{c})(\vec{b}\cdot\vec{d}) - (\vec{a}\cdot\vec{d})(\vec{b}\cdot\vec{c})0\rangle\Big\},
\end{aligned} \tag{4.2}$$

where

$$Z_s = 5, \quad Z_t = 4, \quad Z_u = 4/3.$$

The first element is completely symmetric under permutation, while the other forms are part antisymmetric, which means that their momentum-space wave functions must be antisymmetric to compensate. Thus, when all pions have the same momentum, only the first matrix element form is allowed. The first form is the only one of the three that allows all six pions to have the same flavor.

For the case of six pions, there are 15 isosinglet forms. Again, only the purely symmetric state $|s_6\rangle$ allows all the pions to have the same flavor. For the case of 20 pions, there are over 13 million isosinglet forms of which only the symmetric form allows all pions to have the same flavor. If all forms are equally likely the chance that an N-pion state will lead to all neutral pions is given by

$$P_{\text{all neutral}} = \frac{|\langle s_N|a_0b_0\cdots d_0\rangle|^2}{N_{\text{forms}}}3^{N/2}, \tag{4.3}$$

$$|\langle s_N|a_0b_0\cdots d_0\rangle|^2 = \frac{n_{\text{terms}}^2}{Z_s}\left(\frac{1}{3}\right)^N,$$

where $n_{\text{terms}} = (N-1)!!$ is the number of terms required to construct the purely symmetric state $|s_N\rangle$, and N_{forms} is the number of isosinglet forms which exist for N pions. The number of forms can be found by considering the number of states with projection $m_z = 0$ and subtracting the number of states with projection $m_z = 1$. These numbers are straightforward to calculate by counting the number of ways N values of 1, -1, and 0 can be arranged to form a total of m_z.

The normalization Z_s is difficult to calculate because the various $(N-1)!!$ terms that comprise $|s_n\rangle$ are not orthogonal. For instance,

$$\langle(\vec{a}\cdot\vec{b})(\vec{c}\cdot\vec{d})|(\vec{a}\cdot\vec{b})(\vec{c}\cdot\vec{d})\rangle = 1, \tag{4.4}$$

$$\langle(\vec{a}\cdot\vec{b})(\vec{c}\cdot\vec{d})|(\vec{a}\cdot\vec{c})(\vec{b}\cdot\vec{d})\rangle = \tfrac{1}{3}. \tag{4.5}$$

For an example with N particles, the challenge is to count how many terms have a given number of permutations. Every matrix element can be factorized into products of purely cyclic elements of order N made up of $n = N/2$ dot products,

$$\langle(\vec{a}_1\cdot\vec{b}_1)(\vec{a}_2\cdot\vec{b}_2)(\vec{a}_3\cdot\vec{b}_3)\cdots(\vec{a}_n\cdot\vec{b}_n)|(\vec{a}_1\cdot\vec{b}_2)(\vec{a}_2\cdot\vec{b}_3)\cdots(\vec{a}_{n-1}\cdot\vec{b}_n)(\vec{a}_n\cdot\vec{b}_1)\rangle=\frac{1}{3^{n-1}}. \tag{4.6}$$

We define $C(n)$ as the sum of all cyclic permutations of n dot products, divided by $2n$,

$$C(n)=\frac{1}{3^{n-1}}\frac{1}{2n}. \tag{4.7}$$

The last term along with the factor $(2n)!$ which was divided out in the definition would count the number of ways to arrange $2n$ objects in a cyclic manner. The factor of $1/(2n)$ accounts for the overcounting caused by rotating labels.

We can now express the matrix element normalization factor Z_N as the sum of all possible products of cyclic graphs:

$$Z_N=N!\sum_{n_1,n_2,\cdots s.t. n_1+2n_2+3n_3+\cdots=N/2}\frac{C(1)^{n_1}}{n_1!}\times\frac{C(2)^{n_1}}{n_2!}\cdots\frac{C(N/2)^{n_{N/2}}}{n_{N/2}!}. \tag{4.8}$$

This sum looks identical to the diagrammatic sum used in Eq. (2.7). Thus using the same techniques as in [8] the sum of all diagrams can now be calculated.

If there are no isospin constraints and all isospins are chosen randomly, the probability of all N pions being neutral is $(1/3)^N$. If isospin is constrained to be zero using pairwise constraints, the probability of all the pions being neutral is $(1/3)^{N/2}$. The enhancement due to the pairwise constraint, $P_{\text{all neutral}}/(1/3)^N$, is $3^{N/2}$ and is illustrated in Fig. 6. If the constraint is performed by allowing all N-pion isosinglets to be populated with equal probability, the enhancement calculated with Eq. (4.4) is weaker as can be seen in Fig. 6. The enhancement scales as $N^{1/2}$ for large N.

From viewing Fig. 6, one can sense the importance of constraining the isospin of pions to be a combination

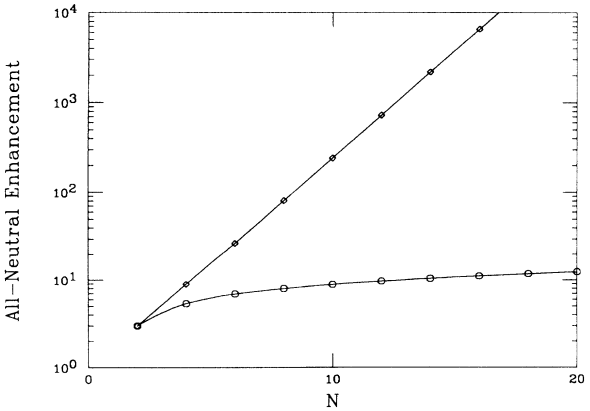

FIG. 6. Constraining N pions to be in an isosinglet singlet enhances the probability of creating all neutral pions. If the constraint is performed pairwise the enhancement to the probability of having all neutral pions is $3^{N/2}$ (diamonds). If all N-particle isoscalar channels are populated equally, the enhancement is weaker (circles).

of many isosinglets rather than constraining the overall isospin. A detailed study of hadronization from gluon-gluon scattering could clear up the question. As two gluons collide subsequent branchings are likely to remain in the gluonic sector. Following a vertex where quark-antiquark pairs are created and then branch out, the resulting mesons must be constrained to an isosinglet. If quarks are exchanged with other branches, the isospin constraint could be spread over more particles. Thus in relativistic heavy-ion collisions, where created quarks are likely to interact many times, assumptions about emitting through isoscalar pairs would be unwarranted.

The existence of heavier resonances also detracts from symmetrization. For instance, an isosinglet branch can decay into two ρ's or two ω's. These isospin structures are included in the list of four- and six-pion isospin forms, but the existence of the resonances enhances the emission in these structures. In most statistical models or string models, pions from resonances account for over half of the total pions. Production in these channels works against large imbalances in the isospin composition. For example, two ω's will always decay into two pions of each flavor.

Several qualitative reasons can be given for explaining why an undue portion of the hadronization of a few pions could be in isosinglet pairs.

(1) Emission of heavy mesons like the ρ and ω through gluonic channels could be suppressed by the fact that they must be produced pairwise to keep the matter in an isosinglet. This penalty for producing more massive mesons would be especially severe if supercooling occurs.

(2) If gluonic matter cools by emitting Pomerons, the Pomerons naturally emit isoscalar pairs.

(3) The chiral condensate, referred to as the σ field in the linear sigma model, could fluctuate rapidly due to the restoration of chiral symmetry. Radiation from the σ field would produce isoscalar pairs.

(4) Since resonances decay away from the collision region, their emission is less enhanced by statistics, reducing the fraction of pions emitted through such channels.

Symmetrization will enhance emission through isoscalar pairs relative to heavier resonances. To illustrate this we consider a binomial multiplicity distribution of isoscalar pairs with an average of 30 and a cutoff of 120. This is shown in Fig. 7 along with symmetrization-weighted distributions. Symmetrization-weighted distributions are found by calculating the average symmetrization enhancement $w(N)$ for N pions:

$$w(N)=\frac{\sum_{n_x+n_y+n_z=N/2}\frac{(N/2)!}{n_x!n_y!n_z!}\omega(2n_x)\omega(2n_y)\omega(2n_z)}{\sum_{n_x+n_y+n_z=N/2}\frac{(N/2)!}{n_x!n_y!n_z!}}, \tag{4.9}$$

where $\omega(n)$ is the symmetrization enhancement for emitting n identical particles described in Eq. (2.7). The symmetrization-weighted multiplicity distribution is then

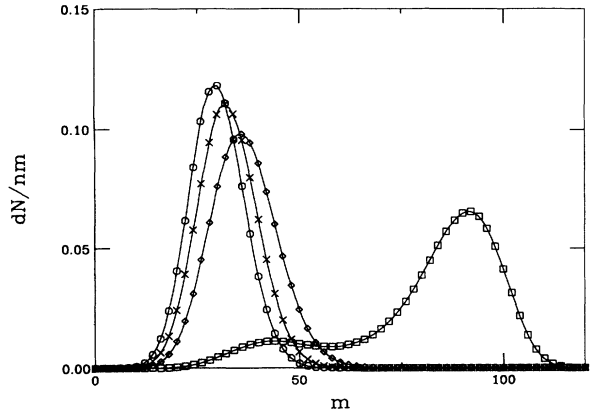

FIG. 7. Multiplicity distributions assuming particles are created pairwise according to a binomial distribution with a cutoff of 120 and a mean of 30 when statistics are neglected (circles). Assuming $\Delta = 3.0$, symmetrization-corrected distributions are shown for $R = c\tau = 1.54$ fm (crosses), 1.22 fm (diamonds), and 1.07 fm (squares). For sufficiently compact phase-space distributions, symmetrization can greatly enhance the probability of high-multiplicity events.

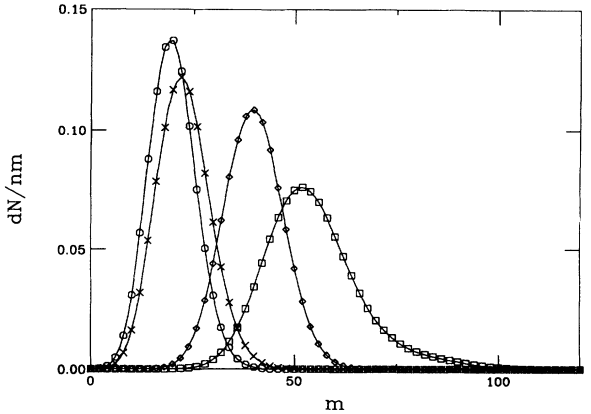

FIG. 8. Multiplicity distributions assuming particles are created pairwise according to a binomial distribution with a cutoff of 120 and a mean multiplicity of either 20 (circles) or 40 (diamonds). Assuming $\Delta = 3.0$ and $R = c\tau = 1.22$ fm, symmetrization-corrected distributions are shown for means of 20 (crosses) or 40 (squares). Significant enhancement to the multiplicity distribution will only occur for distributions with sufficient multiplicity in the base distributions.

$$P(N) = \frac{1}{Z}\frac{(N_{\max}/2)!}{[(N_{\max}-N)/2]!(N/2)!}p^{(N/2)} \times (1-p)^{(N_{\max}-N)/2} w(N) \ , \qquad (4.10)$$

where Z is a normalization and p is the fraction of the maximum $N_{\max}$ usually emitted when symmetrization is neglected. The example in Fig. 7 uses $N_{\max} = 120$ and $pN_{\max} = 30$. Symmetrization corrections were calculated assuming $\Delta = 3$ and that R and τ were chosen to give breakup densities of 0.5 fm^{-3}, 1.0 fm^{-3}, and 1.5 fm^{-3}. One sees that for dense systems emission through isoscalar pairs could be double what one would expect without symmetrization.

The average number of pions emitted in a hadron-hadron collision at 250 TeV energy would be about 40 [15], roughly half the multiplicity of a CENTAURO event. Assuming the incident cosmic ray was to travel through the center of a nucleus instead of colliding with a single nucleon, the expected multiplicity could easily surpass 60. If the expected multiplicity was 60, and half of the pions came through isoscalar pairs, symmetrization could affect the expected multiplicity through the isoscalar-pair channel as shown in Fig. 7. One might then expect 60 pions to be emitted in isoscalar pairs, while another 30 came from other channels such as long-lived resonances. Furthermore, the enhancement into isoscalar-pair channels might come at the expense of emission through other channels.

The most questionable part of the preceding scenario is the assumption that 30 pions could be emitted as isoscalar pairs in the absence of symmetrization. Figure 8 illustrates how the multiplicity distribution is affected assuming 20 or 40 pions was the original average multiplicity in this channel. One sees that, for symmetrization to play a big part in pushing emission through such isoscalar-pair channels, the channel must be responsible for a large fraction of the emission, roughly half, in the absence of symmetrization.

From the calculations described in the next section, one sees that large isospin imbalances can be expected to occur assuming 60 pions are emitted through isoscalar pairs. Despite the arbitrary nature of the examples discussed above, several clear conclusions can be reached. First, the assumption that pions are emitted in isoscalar pairs or perhaps isoscalar quadruples is essential to explaining isospin imbalances. Secondly, if microscopic models could explain roughly half of the pions being emitted through such channels without exploiting symmetrization, symmetrization could enhance emission through these channels such that they comprise a large fraction of the emission. Intuitively, I find the fraction of 1/2 unreasonable, but only by a factor of 2. However, given the much more exotic nature of other explanations where coherent sources are proposed, it does not seem imprudent to proceed given these qualifications. Detailed study of hadronization might clarify this issue.

V. ISOSPIN DISTRIBUTIONS

The principal mystery of CENTAURO's is the isospin imbalance. Several events have been observed with a great excess of charged particles, probably pions, at Chacaltaya [1]. One event with an excess of neutrals has been observed at Mt. Fuji [3]. For the calculation in this section, we assume that 60 pions from isoscalar-pair channels are emitted according to the symmetrization-weighted relativistic Bjorken model described earlier. Certainly some pions would be emitted in other channels with very balanced distributions. But if the 60 isoscalar-pair pions comprise the majority of pions, any large imbalance in their isospin composition would be reflected

in the overall composition.

Isospin weights were calculated by weighting the various isospin compositions by their symmetrization weights:

$$P(n_0) = \frac{1}{Z} \sum_{n_x+n_y=(N-n_0)/2} \frac{(N/2)!}{n_x!n_y!n_0!} \left(\frac{1}{3^{(N/2)}}\right) \times\omega(2n_x)\omega(2n_y)\omega(2n_0). \quad (5.1)$$

For symmetrization to strongly distort the isospin distribution, breakup densities must be large. Figure 9 shows the isospin distribution for three densities, $\rho_{\max} =$ 0.5, 1.0, and 1.5 fm^{-3}. The stopping parameter Δ is taken to be 3.0. The probability of observing a given number of neutral pions out of sixty pions is also shown in Fig. 9 for the case where symmetrization is neglected. One sees that breakup densities must be of the order of $\rho_{\max} \geq 1.0$ fm^{-3} if large imbalances are to occur. One should keep in mind that these values reflect the maximum of the density profile and that average breakup densities would be less than half of these values.

The dependence of the isospin distributions with respect to the stopping parameter was a prime motivation for this study. The simple Gaussian model worked out previously did not incorporate collective expansion. Given the fact that the isospin composition is a global measurement and that many of the pions come from sources with large relative velocities, it was not obvious that the breakup density and temperature were the lone criteria for determining the strength of symmetrization effects.

Figure 10 shows isospin distributions for four values of the stopping parameter assuming R and τ were chosen to yield the same central breakup density. The broadening due to symmetrization is more apparent when Δ is small. But the difference due to different values of Δ is small compared to variation induced by changing the breakup density by 10% or 20%. From this we conclude that, even if pions are emitted over many units of rapidity, symmetrization can strongly increase the chances of events with large imbalances in the isospin composition. However, if Δ is large the value of R and τ necessary to create large breakup densities becomes small. From viewing Fig. 2, one sees that, if R and τ are constrained by the dynamics to never be larger than 1.2 fm, values of Δ larger than 4.0 do not permit $\rho_{\max}$ to exceed 1.0 fm^{-3}. Thus the principal reason that stopping allows stronger symmetrization effects is in the fact that densities become higher for fixed values of R and τ.

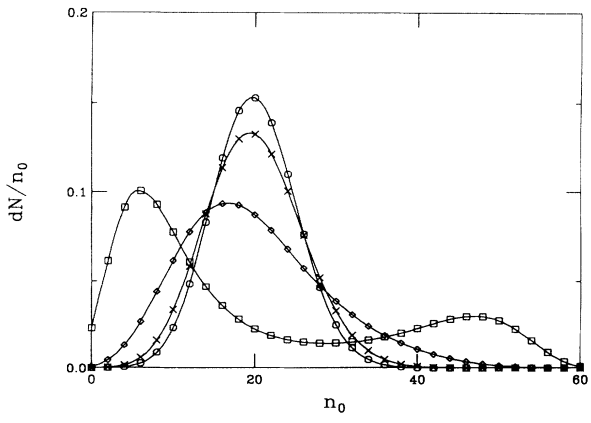

FIG. 9. Given 60 pions, the probability of creating n_0 neutral pions. The probabilities are shown assuming Δ =3.0, and that the maximum breakup densities are 0.5 fm^{-3} (crosses), 1.0 fm^{-3} (diamonds) and 1.5 fm^{-3} (squares). The base distribution where symmetrization is ignored (circles) corresponds to a low break-up density.

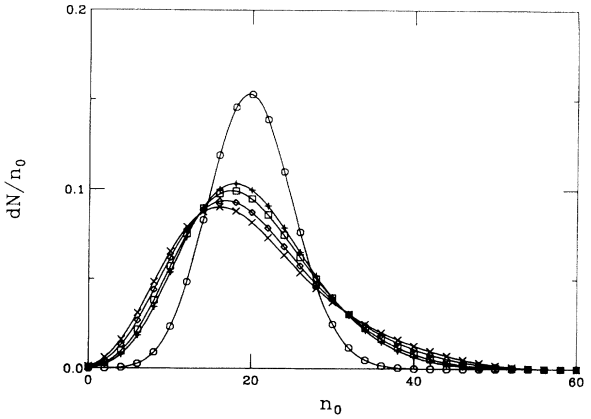

FIG. 10. Given sixty pions, the probability of producing n_0 neutral pions. For each value of Δ the proper time τ and transverse radius R are chosen to correspond to a maximum density of 1.0 fm^{-3}. The rapidity spreads Δ were chosen to be 1.0 (crosses), 3.0 (diamonds), 6.0 (squares), 10.0 (upright crosses), and the base distribution (circles). The effects of symmetrization in broadening the isospin distribution are modestly weaker when there is less stopping, given that τ and R are chosen to yield a fixed maximum density.

VI. CONCLUSIONS

Confident predictions of symmetrization phenomena can not be made without detailed microscopic knowledge which is currently not available. Assuming that CENTAURO phenomena occur when a hadron collides with a nitrogen nucleus in the atmosphere, one needs to know both the expected values of dN/dy. Appropriate parameters for the transverse size are unknown as well, but should certainly be in the neighborhood of 1 fm. If dN/dy, R, and τ are known, we can begin to estimate symmetrization effects. Furthermore, with respect to calculating the chance of observing large isospin imbalances, an understanding of the microscopic mechanism for converting partons (gluons) into hadrons is essential. In particular, one needs to know if a significant fraction of hadrons can be constrained to having been formed in isoscalar pairs, or perhaps quadruples.

Despite the inescapable vagueness due to choosing various parameters, we can reach several firm conclusions.

(1) Symmetrization effects can be strong, even when the sources of particles are spread over several units of

rapidity, provided breakup densities are in the neighborhood of 1.0 fm^{-3}. These high densities are not unphysical given that the cosmic ray hits the center of an atmospheric nucleus.

(2) In order for imbalances of the isospin distribution to occur due to symmetrization, constraining the emission of a large portion of the pions to be isosinglet pairs must be justified. If in the absence of symmetrization effects half of the pions come from such channels, symmetrization can push the fraction emitted in isosinglet pairs to a clear majority.

(3) If symmetrization effects are strong, several signals should exist in the spectra as well. Even in the presence of collective expansion, the dominant species of pion should be more concentrated at low transverse momenta and at midrapidity than the underpopulated species.

(4) Laboratory experiments should be performed with nuclear targets. The most efficient means of producing higher densities is with heavier targets rather than using more energetic beams. If the key to producing CENTAURO behavior is overpopulating phase space, a 2.0 GeV proton beam incident on a fixed lead target might work as well as a 250 TeV cosmic ray incident on a light atmospheric nucleus.

Other models of CENTAURO behavior are based on assumptions that pions are emitted from coherent sources, whereas the calculations contained in this paper are based on assumptions that sources are incoherent. In this sense our goal is to see if spectacular behavior in the laboratory can be explained by models that do not assume new physics. Our answer is yes, given the qualifications that breakup densities are high and that most pions are emitted through isoscalar pairs. The first assumption does not seem unreasonable, especially if it can be shown that CENTAURO behavior occurs only when phase-space densities are high. Given the sort of statistics one would expect from terrestrial experiments, phase-space densities can be inferred from interferometry and singles measurements [16]. The second assumption regarding isospin constraints is more questionable. Detailed microscopic models of hadronization might clarify the issue. It is essential that this line of research is followed. Before CENTAURO behavior can be shown as proof of novel mechanisms, it must be demonstrated that such behavior is not the result of common mechanisms combined with the indisputable fact that pions are bosons.

ACKNOWLEDGMENTS

Discussions with Vladimir Zelevinsky and Brett Carlson were greatly appreciated. This work was supported by NSF Grant No. PHY-925355, and NSF Grant No. PHY-9017077.

[1] C.M.G. Lattes, Y. Fujimoto, and S. Hasegawa, Phys. Rep. **65**, 151 (1980).
[2] K. Rajagopal and F. Wilczek, Nucl. Phys. **B399**, 395 (1993).
[3] J.D. Bjorken, K.L. Kowalski, and C.C. Taylor, SLAC report 1993.
[4] C.S. Lam and S.Y. Lo, Phys. Rev. Lett. **52**, 1184 (1984).
[5] C.S. Lam and S.Y. Lo, Phys. Rev. D **33**, 1336 (1986).
[6] C.S. Lam and S.Y. Lo, Int. J. Mod. Phys. A **1**, 451 (1986).
[7] B. Lacroix and C.S. Lam, Can. J. Phys. **66**, 34 (1988).
[8] S. Pratt, Phys. Lett. B **301**, 159 (1993).
[9] S. Pratt and V. Zelevinsky, Phys. Rev. Lett. **72**, 816 (1994).
[10] J.D. Bjorken, Phys. Rev. D **27**, 1327 (1983).
[11] K. Geiger, Nucl. Phys. **B369**, 600 (1992).
[12] K. Geiger, Phys. Rev. D **47**, 133 (1993).
[13] X.N. Wang, Phys. Rev. D **44**, 3501 (1991).
[14] P. Carruthers, Phys. Rev. Lett. **50**, 1179 (1983).
[15] Particle Data Group, Phys. Lett. B **239**, III.71 (1990).
[16] G.F. Bertsch, Phys. Rev. Lett. **72**, 2349 (1994).